Asian Journal of Chemistry; Vol. 29, No. 5 (2017), 1108-1112

ASIAN JOURNAL OF CHEMISTRY

https://doi.org/10.14233/ajchem.2017.20441

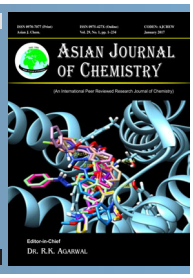

Preparation, Characterization and Photocatalytic Study of Sn/TiO_2-Laponite

IS FATIMAH

Department of Chemistry, Universitas Islam Indonesia, Kampus Terpadu UII, Jl. Kaliurang Km 14, Sleman, Yogyakarta, Indonesia

Corresponding author: E-mail: isfatimah@uii.ac.id

Received: 9 December 2016; *Accepted*: 4 February 2017; *Published online*: 10 March 2017; AJC-18309

In this research, synthesis of Sn-doped TiO_2/laponite and its application in photodegradation of rhodamine B was conducted. Material preparation was performed by two steps; TiO_2 pillarization onto laponite structure and Sn dopping by mean microwave assisted dispersion. The effects of each step on the physical and chemical properties of the materials are reported. Sample was characterized by X-ray powder diffraction, specific surface area measurement by gas sorption analyzer, scanning electron microscopy and ultraviolet-visible diffuse reflectance spectroscopy. Results showed that Sn-dopped TiO_2/laponite was succesfully synthesized with the formation of anatase phase homogeneously supported in laponite as matrix. Increasing specific surface area and the effective band gap energy at around 3.22 eV were the important character as photocatalyst. Subsequent photocatalytic studies of the degradation of rhodamine B under UV irradiation demonstrated that the modification had a positive effect on photocatalytic performance whereas the addition of 0.4 % Sn to TiO_2/laponite enhanced photocatalytic activity. Compared to bulk-TiO_2, TiO_2/Laponite sample itself showed atom efficiency in that the degradation rate of rhodamine B by 10 % Ti was comparable with pure TiO_2. Kinetics study on rhodamine B and the relationship with physico-chemical character of photocatalyst was also the focus of this study.

Keywords: Laponite, Photocatalyst, Pillared clay, TiO_2.

INTRODUCTION

The use of semiconductors as materials for photocatalytic applications has been intensively studied since Fujishima and Honda reported their water electrolysis work in 1972. Development of photocatalytic reaction for environmental applications was then becomes interesting topic. Among some metal oxide semiconductor, titanium dioxide (TiO_2) based nanoparticles is the popular material. Enhancement of photocatalytic properties of TiO_2 by such metal dopping and supporting TiO_2 in a porous inorganic material are schemes for this study. Photocatalysis is one of developing techniques in such application including in environmental protection. Photodegradation of toxic chemicals by photocatalytic degradation is one example technique for safer mechanism of toxic removal compared to other method such as adsorption. By those wide range of the application photocatalysis, photocatalyst is the key role in the mechanism. Among some potential semiconductors for this application, TiO_2 is chosen as potential material refers to its cost and non-toxicity with sufficient and appropriate band gap energy. Improvement on the photocatalytic activity of TiO_2 can be conducted by other metal dopping into the structure and also the formation of material in nanoparticles form and also by dispersing TiO_2 in a stable and high performance solids [1-4]. Many investigations have been carried out on the supporting TiO_2 onto porous materials refer to their goal to enhance photocatalysis which is also related to adsorption mechanism involved [4-6]. Another strategy of TiO_2 modification were also conducted by dopping the TiO_2 structure with some metal and metal ions such as Co, Sn and Cu [7]. Tin is a popular metal related for the significantly improvement on photocatalytic activity of some photocatalyst semiconductor materials [8-11]. By considering these results this research aimed to innovate the improvement of TiO_2 photoactivity by dispersing into clay matrix combined with Sn dopping onto the dispersed materials. Physico-chemical characterization of material and its relationship in the activity was studied in a dye degradation reaction. Rhodamine B (RhB) was utilized as molecule model.

EXPERIMENTAL

Materials used in this research consist of Laponite RD supported by Southern Clay Inc., rhodamine B, isopropanol, titanium isopropoxide, $SnCl_2 \cdot 2H_2O$ are purchased from Merk-Millipore.

Synthesis and characterization of Sn-dispersed titanium oxide pillared laponite (Sn/Ti-LAP): Synthesis of Sn/Ti-LAP was conducted by two main steps; TiO_2 pillarization

onto laponite to produce titanium-pillared laponite (Ti-LAP) and Sn dispersion into Ti-LAP. The pillarization was conducted by dispersing of TiO_2 precursor solution formed by dissolving titanium isopropoxide with isopropanol solvent followed by stirring for 4 h. The precursor was then slowly titrated into laponite suspension in water (5 wt %) followed by stirring for a night. Theoretical content of titanium in the mixture was set up at 10 mmol/g clay. Filtration and neutralization were conducted for derived mixture to get solid before drying and calcination at 400 °C for 5 h under air flow and from these steps the material was designated as Ti-LAP. Tin dispersion into TiO_2-LAP was conducted by impregnating tin from $SnCl_2{\cdot}2H_2O$ solution. The solution was mixed and stirred with Ti-LAP powder for a night before water solvent removal to get Sn/Ti-LAP. Sn content was theoretically set up at 0.4 wt %.

Characterization of Sn/Ti-LAP: Raw laponite (LAP), Ti-LAP and Sn/Ti-LAP were characterized using Hitachi Powder X-ray diffractometer (PXRD) X6000 for the phase purity and crystallinity of the materials. The diffraction patterns were recorded at room temperature using CuK_α (1.541 Å) radiation with nickel filter in the 2θ range 3-70° at a scan rate of 2° min^{-1}. SEM-EDS, Hitachi-3000 was utilized to analyze the morphological features and particle size of materials and also elemental analysis of materials. The diffuse reflectance-UV-visible (DRUV-Vis) spectrum was recorded on JASCO 6000 UV-visible spectrophotometer. The surface parameters of materials including specific surface area, pore volume and pore radius of the sample were recorded using NOVA 1200e gas sorption analyzer.

Photocatalytic activity: The photocatalytic experiments were carried out using a batch glass reactor completed with UVA Lamp (Fig. 1). A typical experiment contains 250 mg of photocatalyst dispersed in 500 mL of rhodamine B (RhB) solution. The reaction mixture was stirred vigorously using magnetic stirrer for entire time span of the experiment. Prior to irradiation, the reaction mixture was stirred for 15 min to ensure the establishment of adsorption/desorption equilibrium. In order to ensure photocatalysis occurred over the prepared materials, such varied process were treated consist of adsorption, photolysis, photocatalysis and photooxidation process. The detail of the process are as follow:

Adsorption: with catalyst addition without UV and H_2O_2.
Photolysis: without catalyst addition, with UV, without H_2O_2.
Photocatalysis: with catalyst addition, with UV, without H_2O_2.
Photooxidation: with catalyst addition, with UV, with H_2O_2.

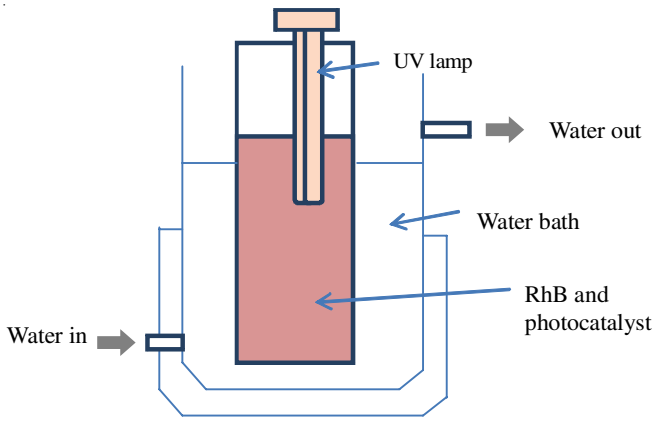

Fig. 1. Scheme of photocatalytic reactor

Photodegradation rate was found from the change of rhodamine B concentration measured by colorimetric method using UV-visible spectrophotometer HITACHI U 2010.

RESULTS AND DISCUSSION

Characterization: Laponite is one of the clay minerals within the smectite class which contains 2:1 silica-alumina structure and having swelling properties. In the synthesis of Sn/Ti-LAP, two-steps methods were applied consist of TiO_2-pillarization and tin dispersion onto TiO_2-pillared laponite. As many pillarization procedure conducted for several clays particularly smectite clay, there will be an increasing basal spacing d_{001} of the smectite which contribute to enhance the specific surface area as well as the space in interlayer to be filled with other functional molecule or metal ion (Fig. 2).

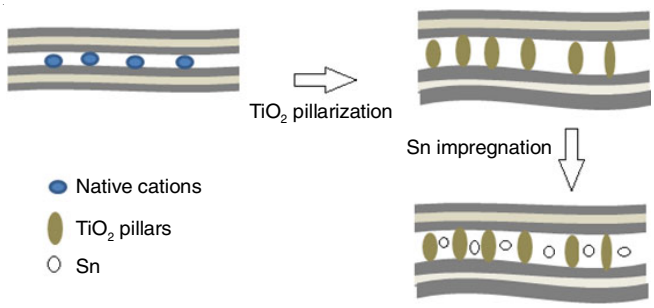

Fig. 2. Schematic representation of Sn/Ti-LAP preparation

X-ray diffraction was used to analyze the change of clay's structure and the result is presented in Fig. 3. The XRD of laponite sample shows the reflections at 2θ = 6.8, 19.9 and 35.5° respect to the specific reflections of laponite structure of d_{001}, d_{002} and d_{006} spaces [12,13]. After pillarization the d_{001}

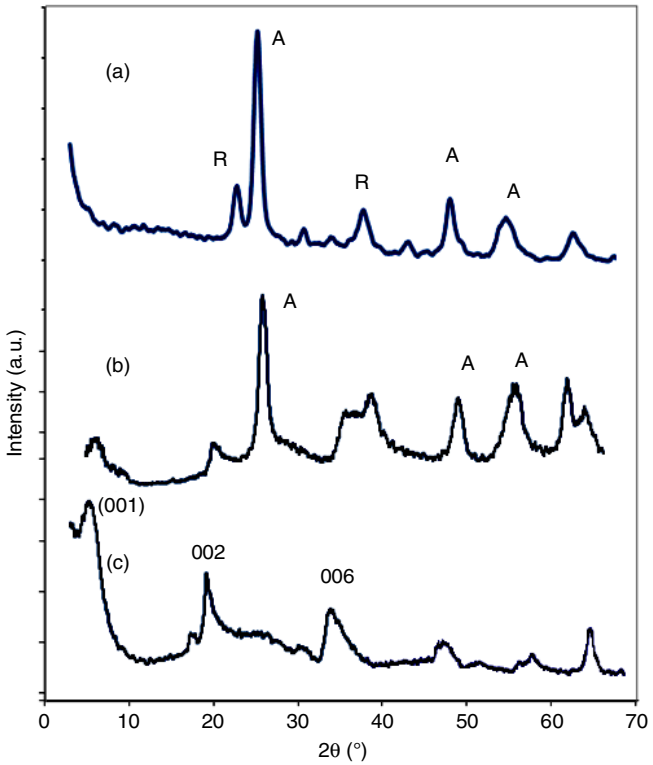

Fig. 3. XRD pattern of materials (a) Sn/Ti-LAP (b) Ti-LAP (c) LAP

basal spacing which is correspond to 1.48 nm was slightly shifted into lower angle which is related to the increasing basal spacing value of 1.49 nm. Another important thing from the pillarization is the presence of some peaks ascribed to the TiO_2 crystalline anatase phase at 2θ = 25.367°, 48.16° and 55.20° which are attributed to the 101, 112, 105 (JCPDS Card no. 78-2486). With Sn modification on Ti-LAP to form Sn/Ti-LAP, the reflections exhibit the change of TiO_2 formation from only anatase phase into the combination of anatase and rutile by the presence of reflections at 2θ = 22 and 37.8° (JCPDS file No. 21-1276) [14,15]. The similar transformation was also reported by previous research in that the presence of tin accelerate the transformation of anatase to rutile [7].

The modification onto laponite affect to the surface profile and porosity of the solid as expressed by surface parameters of specific surface area, pore volume and pore radius listed in Table-1. Adsorption-desorption profile of the materials show the evolution on porous structure in that the formation of dominantly microporous structure was found by pillarization and tin dispersion onto laponite (Fig. 4).

TABLE-1
SURFACE PARAMETERS OF MATERIALS

Parameter	LAP	Ti-LAP	Sn/Ti-LAP
Specific surface area (m^2/g)	69.76	92.05	88.95
Pore volume (cc/g)	5.58×10^{-2}	7.65×10^{-2}	6.23×10^{-2}
Pore radius (Å)	14.04	15.20	14.78

The change of surface profile was also indicated by SEM profile (Fig. 5). Rougher surface appearance of Ti-LAP and Sn/Ti-LAP is the proof of titania dispersion on surface while there is no significant difference after tin dispersion into Ti-LAP.

Considering that the main purpose of titania pillarization and tin dispersion is to enhance photocatalytic activity, diffuse reflectance UV-visible spectrophotometric analysis to the materials was conducted and the spectra is presented in Fig. 6. The existence of TiO_2 anatase is expressed by the higher absorbance value at almost all wavelength range and also the band gap energy value of 3.20 eV while laponite give no specified edge wavelength correlated with specific band gap energy. Furthermore the band gap value of Sn/Ti-LAP is 3.19 eV which is lower than that of Ti-LAP. The formation of rutile detected from the XRD analysis is related to this reducing band gap value. However the reflection of Sn/Ti-LAP is higher than Ti-LAP in all range of wavelength.

Photocatalytic activity: In general kinetics degradation of rhodamine B (Fig. 7) demonstrated the increasing degradation rate by both modifications; TiO_2-pillarization and Sn dispersion. The increasing degradation rate from photodegradation compared to adsorption and photolysis are also confirmed the enhancement of photocatalytic activity of the materials (Fig. 8).

By comparing rhodamine B reduction by adsorption process, it is found that the adsorption capability of Ti-LAP is similar with Sn/Ti-LAP but then with UV illumination, the addition of H_2O_2 in photooxidation affect to accelerates the rhodamine B degradation due to the increasing rate of $^{\bullet}OH$ formation. Furthermore, initiated $^{\bullet}OH$ will oxidize target molecule in the scheme of cleavages of functional group of rhodamine B structure.

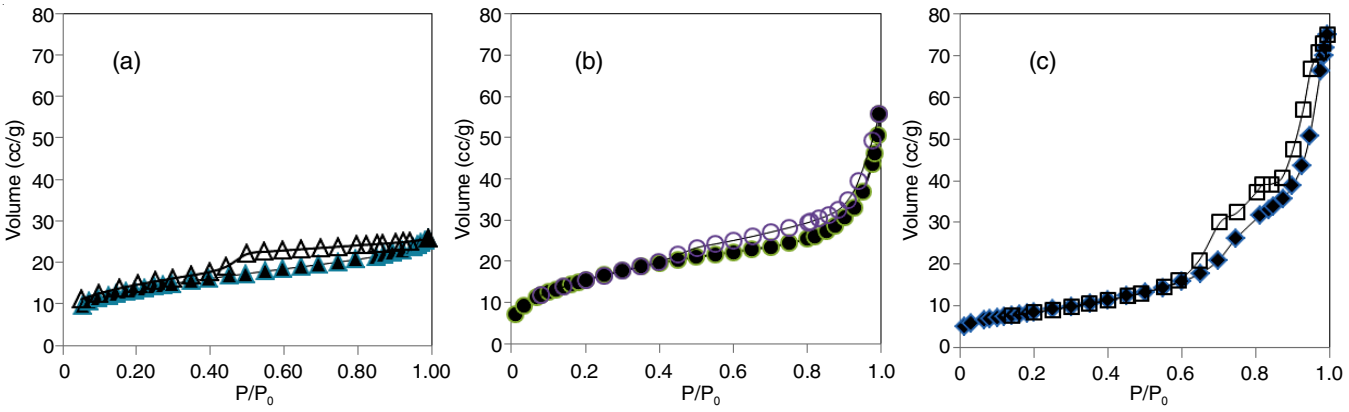

Fig. 4. Adsorption-desorption patterns of (a) LAP (b) Ti-LAP (c) Sn/Ti-LAP

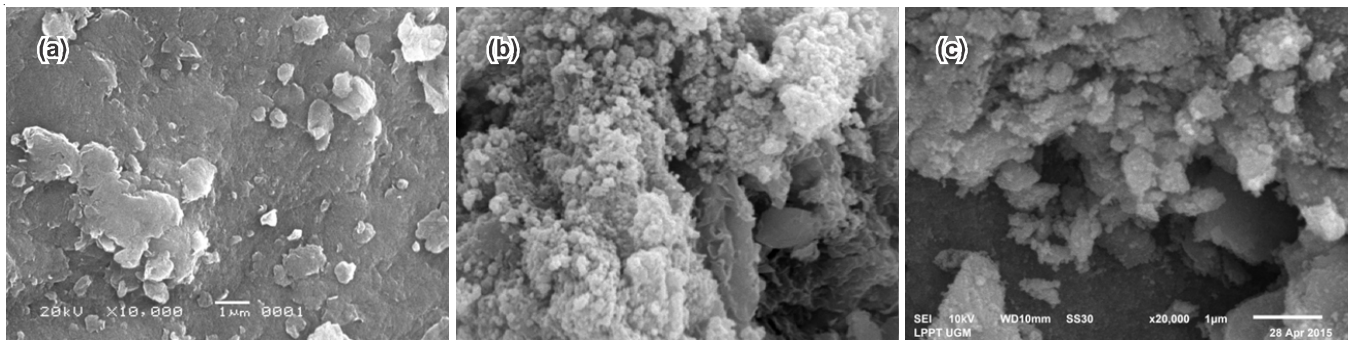

Fig. 5. SEM profiles of (a) LAP (b) Ti-LAP (c) Sn/Ti-LAP

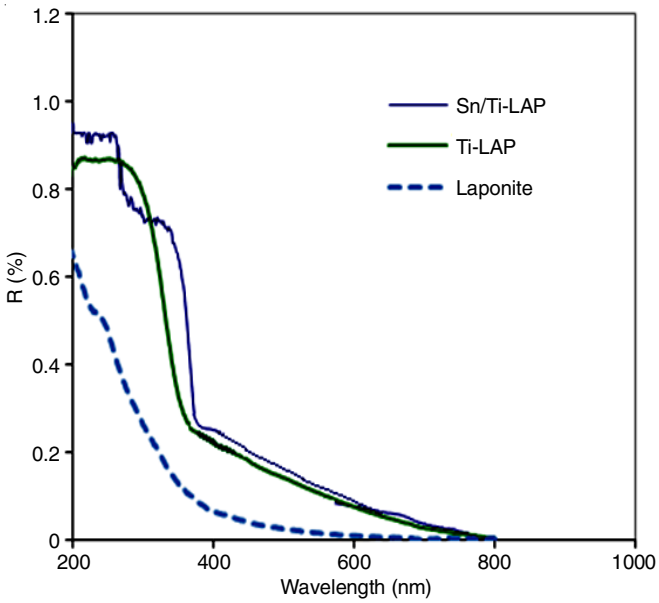

Fig. 6. DRUV-visible spectra of materials

$$H_2O_2 + UV \longrightarrow 2\ ^{\bullet}OH$$

The mechanism consistence to photolysis kinetic data. The reduction of rhodamine B by photolysis is relatively low and similar to as the result from adsorption. The oxidation of rhodamine B by photolysis is related to radical formation from the interaction between UV light with both the solvent (H_2O) and molecule itself which is not as rapid as the formation from H_2O_2 illumination. Increasing rate by photocatalysis was due to the radical formation by the interaction between photocatalyst and UV light.

The study on photocatalyst stability was conducted by evaluating the degradation rate of rhodamine B by photooxidation over reused photocatalyst of Ti-LAP and Sn/Ti-LAP. Comparison on the rate over two materials at first until 4th use is depicted in Fig. 9. It is reasonable that Sn/Ti-LAP is more stable compared with Ti-LAP in that the rate is remain constant. It is also mean that the presence of tin in the composite is not released in the treated solution so the photocatalytic enhancement was still maintained.

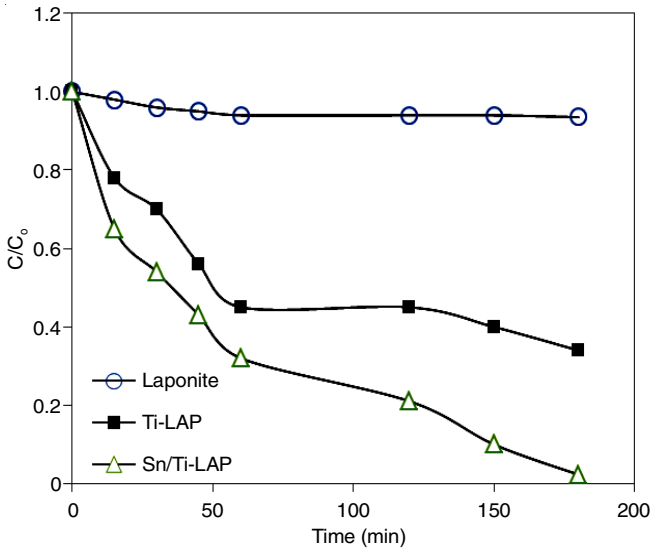

Fig. 7. Kinetics of rhodamine B degradation over varied materials using photooxidation process ([RhB] = 10^{-4} M)

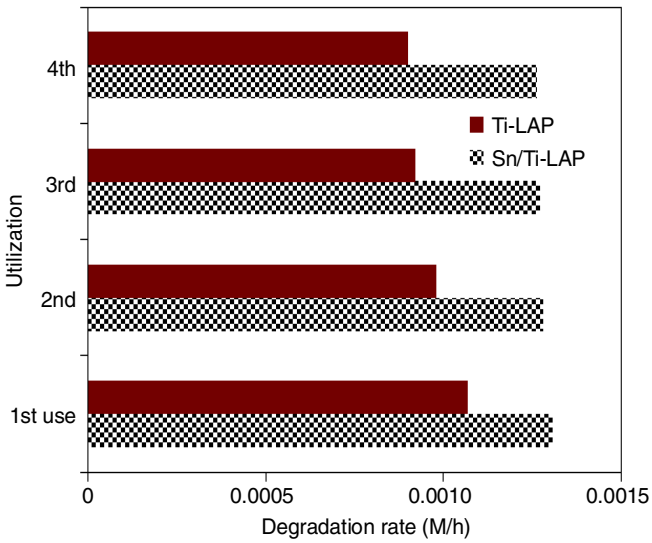

Fig. 9. Degradation rate by reused photocatalyst

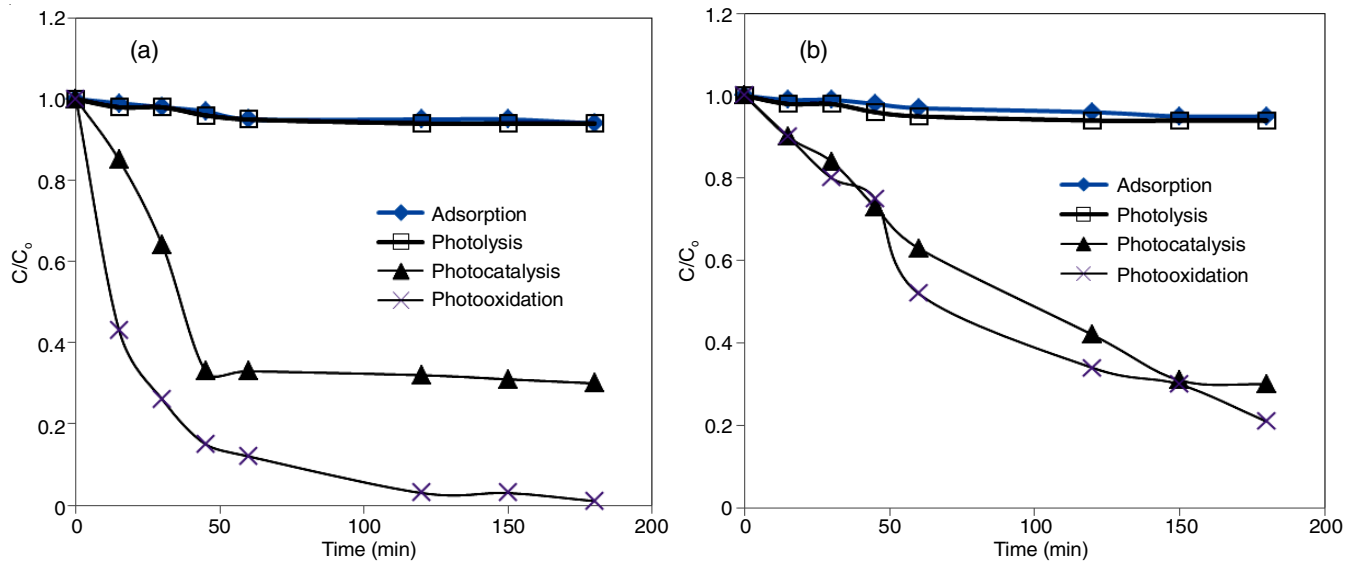

Fig. 8. Kinetics of rhodamine B degradation over varied process using (a) Sn/Ti-LAP (b) Ti-LAP

Conclusion

The photocatalyst of tin dispersed into titanium pillared aponite was successfully prepared. The physico-chemical character measurement of materials indicated the formation of anatase and rutile phases in the composite. Diffuse reflectance-UV-visible spectra and photocatalytic activity test show that the increasing photocatalytic activity of titanium pillared laponite by tin dispersion.

ACKNOWLEDGEMENTS

The author acknowledge to Chemistry Department, Universitas Islam Indonesia, for providing the facilities for the research through Material and Electrochemistry for Energy and Environment Research Excellencies.

REFERENCES

1. N. Yao, S. Cao and K.L. Yeung, *Micro. Meso. Mater.*, **117**, 570 (2009); https://doi.org/10.1016/j.micromeso.2008.08.020.
2. C. Liu, Z. Chen, Z. Miao, F. Chen, C. Gu, M. Huang and X. Zhao, *Procedia Eng.*, **27**, 557 (2012); https://doi.org/10.1016/j.proeng.2011.12.487.
3. M.N. Chong, Z.Y. Tneu, P.E. Poh, B. Jin and R. Aryal, *J. Taiwan Inst. Chem. Eng.*, **50**, 288 (2015); https://doi.org/10.1016/j.jtice.2014.12.013.
4. L. Ma, J. Ji, F. Yu, N. Ai and H. Jiang, *Micropor. Mesopor. Mater.*, **165**, 6 (2013); https://doi.org/10.1016/j.micromeso.2012.05.005.
5. M.N. Chong, Y.J. Cho, P.E. Poh and B. Jin, *J. Clean. Prod.*, **89**, 196 (2015); https://doi.org/10.1016/j.jclepro.2014.11.014.
6. Q. Sun, X. Hu, S. Zheng, Z. Sun, S. Liu and H. Li, *Powder Technol.*, **274**, 88 (2015); https://doi.org/10.1016/j.powtec.2014.12.052.
7. M. Khairy and W. Zakaria, *Egyptian J. Petrol.*, **23**, 419 (2014); https://doi.org/10.1016/j.ejpe.2014.09.010.
8. B. Sun, T. Shi, Z. Peng, W. Sheng, T. Jiang and G. Liao, *Nanoscale Res. Lett.*, **8**, 462 (2013); https://doi.org/10.1186/1556-276X-8-462.
9. F. Sayilkan, M. Asiltürk, P. Tatar, N. Kiraz, S. Sener, E. Arpaç and H. Sayilkan, *Mater. Res. Bull.*, **43**, 127 (2008); https://doi.org/10.1016/j.materresbull.2007.02.012.
10. C. Wu, L. Shen, H. Yu, Q. Huang and Y.C. Zhang, *Mater. Res. Bull.*, **46**, 1107 (2011); https://doi.org/10.1016/j.materresbull.2011.02.043.
11. Y. Liu, X. Chen, Y. Xu, Q. Zhang and X. Wang, *J. Nanomater.*, **Article ID 381819** (2014); https://doi.org/10.1155/2014/381819.
12. S. Yang, J. Nam and Y. Kim, *Bull. Korean Chem. Soc.*, **35**, 1218 (2014); https://doi.org/10.5012/bkcs.2014.35.4.1218.
13. T. Batista, A. Chiorcea-Paquim, A.M.O. Brett, C.C. Schmitt and M.G. Neumann, *Appl. Clay Sci.*, **53**, 27 (2011); https://doi.org/10.1016/j.clay.2011.04.007.
14. S. Bagheri, K. Shameli and S.B.A. Hamid, *J. Chem.*, **Article ID 848205** (2013); https://doi.org/10.1155/2013/848205.
15. C. Wang, H. Shi, P. Zhang and Y. Li, *Appl. Clay Sci.*, **53**, 646 (2011); https://doi.org/10.1016/j.clay.2011.05.017.